ISSN 1840-4855
e-ISSN 2233-0046

Original scientific article
http://dx.doi.org/10.70102/afts.2025.1732.075

GEOCHEMICAL AND GEOLOGICAL STUDIES OF OIL SHALES IN AB KASEH SECTION, KOUHRANG COUNTY, CHAHARMAHAL AND BAKHTIARI PROVINCE, IRAN

Milad Tahmasebi[1], Farhad Ehya[2*], Ghodratollah Rostami Paydar[3]

[1]Department of Geology, Behbahan Branch, Islamic Azad University, Behbahan, Iran.
e-mail: milad.tahmasebi66@gmail.com, orcid: https://orcid.org/0009-0005-3989-9417
[2]Department of Geology, Behbahan Branch, Islamic Azad University, Behbahan, Iran.*
e-mail: ehya@behiau.ac.ir, orcid: https://orcid.org/0000-0002-0474-3958
[3]Department of Geology, Ahvaz Branch, Islamic Azad University, Ahvaz, Iran.
e-mail: rostamigsi2006@gmail.com, orcid: https://orcid.org/0000-0001-8406-6688

Received: December 20, 2024; Revised: January 23, 2025; Accepted: February 14, 2025; Published: March 28, 2025

SUMMARY

This study investigates the geochemistry of oil shales from the Ab Kaseh section in western Kohrang, Chaharmahal and Bakhtiari Province, Iran. Ten shale samples were collected for geochemical analyses, including Rock-Eval pyrolysis and XRF/ICP analyses. Ten thin sections were also prepared for petrographic analysis. A stratigraphic column and depositional model were constructed based on microfacies characteristics. Results indicate that the oil shales formed in a marine, reducing environment within the Tethys Ocean. However, due to discontinuous sedimentation and insufficient heat supply, the shales never reached the necessary thermal maturity for hydrocarbon generation. Hydrocarbon generation is only achievable through artificial heating (pyrolysis). Rock-Eval pyrolysis data revealed high hydrocarbon potential, with TOC values exceeding 2%, indicating excellent source rock quality. The kerogen type is classified as Type II, suggesting a predominantly oil-prone nature with good to excellent petroleum potential. The samples are situated at the early stage of the oil window (late diagenesis/early catagenesis) and show no potential for gas generation. XRF and ICP analyses showed elevated concentrations of heavy metals (Ni, Pb, Rb, Sr, V, W, Zr, Zn) and rare earth elements (Ba, Ce, Co, Cr, Cu, Th, Nb, Mo, U) within the oil shales. Potential sources of these elements include organic matter, detrital material, seawater, submarine volcanism, and biogenic sources. In the Ab Kaseh section (Saraglu Formation), elements such as Sr and P may have biogenic origins. Ti, Al, and Si, constituents of oxide and clay minerals, have a detrital origin. The origin of Ni, U, W, and Cr is likely linked to organic matter and adsorption onto clay minerals. Positive correlation between P and TOC supports a biogenic origin for P in the Ab Kaseh section. Conversely, the negative correlation between Sr and TOC suggests a non-biogenic source for Sr. A positive correlation between Ni and TOC was also observed. The negative correlation between U and both SiO2 and Al2O3 indicates an uncertain origin for U, but organic matter and clay minerals likely contributed to its enrichment.

Key word: *rock-eval pyrolysis, oil shale, ab kaseh section, saraglu formation, geochemical analysis.*

INTRODUCTION

The studied area of oil shales is located in the Central Zagros region, near the Zardkuh Bakhtiari, in the steep and rugged terrain of western Chaharmahal and Bakhtiari Province [3]. The oil shales of the Ab Kaseh section represent a diverse group of sedimentary rocks that serve as oil source rocks (kerogen) and contain both organic and inorganic materials [10]. The organic matter within these shales has not reached thermal maturity and migration due to insufficient burial depth, resulting in a lack of oil generation. However, oil can be extracted through pyrolysis, a process involving heating and distillation [31].

By conducting geochemical analyses of the oil shales in this area, the oil potential and hydrocarbon content of these reserves can be determined. The Rock-Eval pyrolysis will provide insights into the thermal conditions necessary for oil generation, kerogen types, hydrocarbon types, potential oil yield, and the quality of the source rock [25][16]. The concentrations of rare earth elements and heavy metals were also evaluated and discussed [9]. Heavy metal concentrations were determined using the XRF method, while the concentrations of rare earth elements were assessed using ICP techniques [2]. Following the results obtained from the analyses, the data for the Ab Kaseh section were recorded in a tabular format for ease of writing, with the samples denoted by the label "AB." It should be noted that no geological studies have previously been conducted in this area, and there was no information [6] available regarding the petrography and relative age of the oil shale strata [13][20]. Thus, this research also includes a petrographic study, with ten thin sections prepared from the Ab Kaseh samples [4]. These were analyzed for depositional environment and rock classification using the [15] and Folk (1965) methods, leading to the construction of a stratigraphic column and depositional model for the Ab Kaseh section [23].

LOCATION AND GEOLOGICAL ANALYSIS OF THE REGION

The Zagros Basin is one of the significant tectonic units of Iran, situated parallel to the Sanandaj-Sirjan zone and the western thrust of the Zagros range [5]. The southeastern limit of this zone is defined by the Oman Mountains, while the western boundary is marked by the Arabian Shield, and the eastern limit is defined by the Minab Fault (Map 1).

Various classifications have been proposed for the Zagros Zone, with the most notable being the Stöcklin classification [27]. This classification subdivides the Zagros Basin into three separate structural units, which include:

- Khuzestan Plain
- Folded Zagros (External Zagros)
- Elevated Zagros (Internal Zagros)

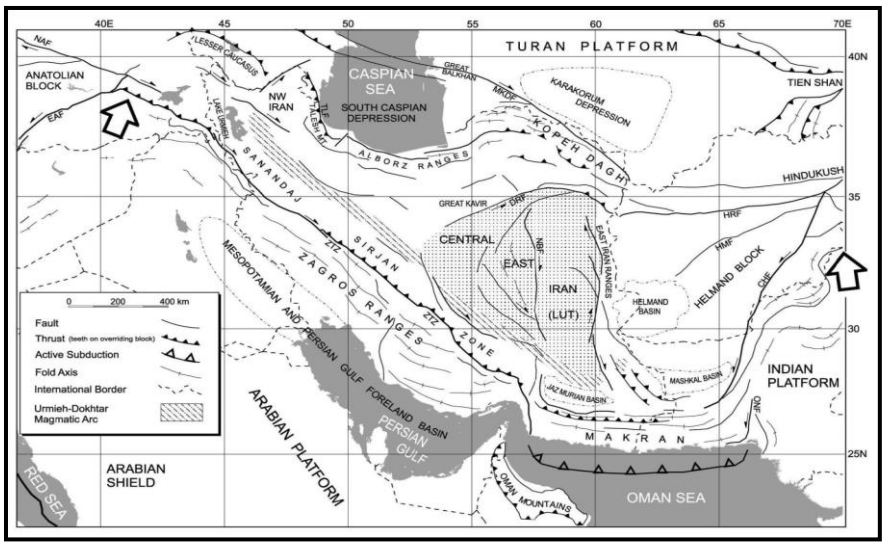

Map 1. Tectonic Structure of Iran [7]

The geographical location and geological characteristics of the structural features of Chaharmahal and Bakhtiari Province, as well as the studied area, encompass parts of the Central Zagros region and the Sanandaj-Sirjan zone (Mohajel, M. 2003). Since the orientation of these structural units is northwest-southeast, an approximate transverse section of them includes this province.The studied section is located in the western part of the Kouhrang region within Chaharmahal and Bakhtiari Province, with geographic coordinates of 32° 34’ 32.73" latitude and 49° 55’ 3.80" longitude. This area falls within the geological map of Shahrekord at a scale of 1:250,000 (Map 2). In terms of Zagros geological divisions, it is situated in the High Zagros zone and the Central Zagros region.

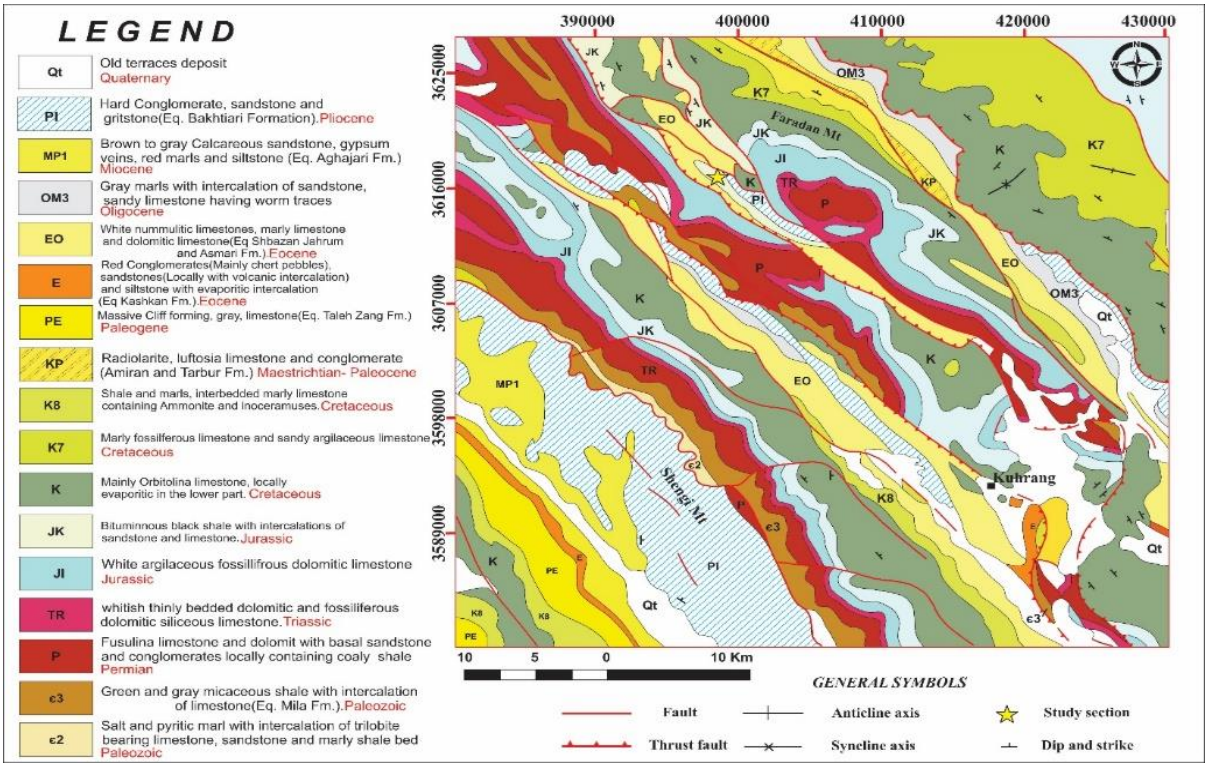

Map 2. Geological Map Redrawn from the Studied Area

Oil shales, as organic mineral resources, are found in various rock formations of the Zagros region in Chaharmahal and Bakhtiari Province [8]. Among the most significant of these are the Hormuz Formation, the Dalana Formation, and the formations associated with the Jurassic-Cretaceous period, with the Saraghal Formation being particularly noteworthy for its considerable reserves [17]. The outcrops of these oil shales are predominantly located in the western part of the province and within the High Zagros region. This phenomenon can be attributed to the activity of major faults in the High Zagros area, such as the Ardil and Zardkuh faults, which have resulted in vertical displacements of approximately 6,000 meters [30].

Although extensive outcrops of oil shales are evident at the erosional cut of rivers, sampling and work in these steep valleys pose significant risks [21]. Therefore, more suitable locations for sampling and further investigation are the outcrops along the ridges adjacent to fault lines, particularly in the vicinity of western Kouhrang County (western Chaharmahal and Bakhtiari Province). This area was identified as the optimal site for the selection of study sections (Map 3).

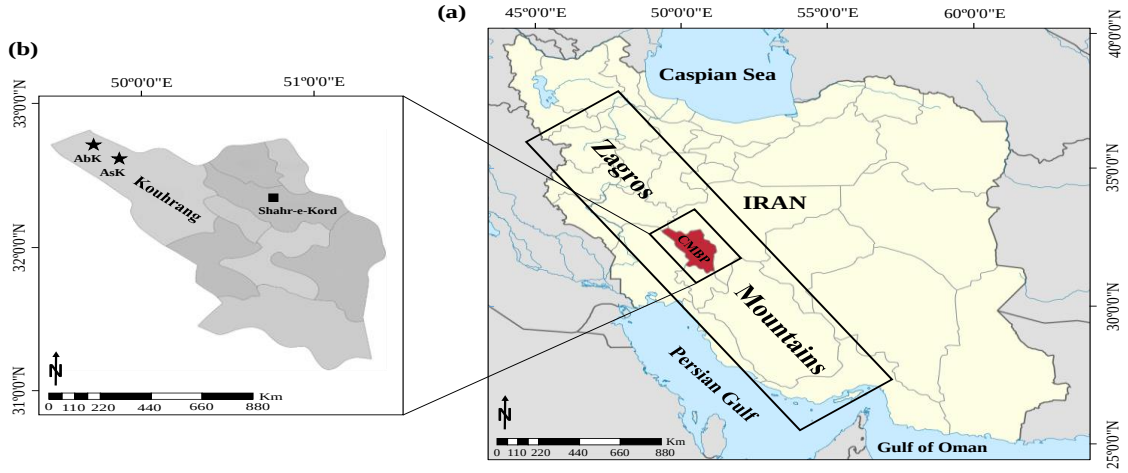

Map 3. Location of Chaharmahal and Bakhtiari Province and the Studied Section on the Map of Iran

The oil shales in this region belong to the Saraghal Formation, which dates back to the lower Jurassic period. These sediments were deposited in a relatively deep sea, which confirms that they are remnants of the Tethys Ocean [33]. The color of these shales is extremely dark to grayish, with a strong and unpleasant odor, and often accompanied by bands of pyrite (Figure 1).

Figure 1. Close-up Image of Oil Shales from the Water Basin Exposure in Central Zagros

Evidence suggests that the Jurassic sediments in this area (Central Zagros) were formed in an open sea of the homoclinal ramp type. In this marine environment, the Saraghal Formation was deposited simultaneously in deeper regions, while in the shallow ramp and tidal flat areas, sediments of the Neyriz Formation were formed. This interdigitation of facies is indicative of their concurrent development within a single sedimentary basin, namely the Tethys Ocean [26].

METHODOLOGY

This research investigated the Jurassic oil shales in western Chaharmahal and Bakhtiari Province, focusing on the stratigraphic analysis of the Ab Kaseh Pass. The initial geological maps of Iran did not specifically assign a formation to the Ab Kaseh Pass. Field surveys identified optimal outcrops for study. After selecting the study section, systematic measurements and sampling were conducted. Following preliminary investigations, geological maps and field surveys guided the selection of the best outcrops from the mineral deposit [11]. The location of oil shale within the host rock was then assessed, and samples were collected for geochemical analysis. This stage included precise measurements of the actual thickness of the oil shale sediment sequence at each section.

Selected samples were sent to geochemical laboratories for preparation and analysis to determine hydrocarbon content, heavy metals, trace elements, economic viability, and formation processes. While various geochemical methods exist for analyzing shales, XRF was employed to determine heavy metal concentrations, ICP for trace elements, and Rock-Eval pyrolysis for hydrocarbon generation potential and hydrocarbon yield.

The Research Comprised Three Main Axes

a. Field studies: Observations, sample collection, photography, and measurements. b. Geochemical analysis: Data obtained using Rock-Eval pyrolysis, X-ray Fluorescence Spectroscopy (XRF), and Inductively Coupled Plasma-Atomic Emission Spectroscopy (ICP). c. Literature review: Collection of relevant articles, books, reports, and other materials.

In total, 20 oil shale samples were collected from the Ab Kaseh Pass section and subjected to the aforementioned analyses. Geochemical analysis determined trace element and heavy metal concentrations, overall hydrocarbon potential, and provided data for microscopic section preparation [36]. Sedimentary environment analysis and discussions followed. Finally, obtained data was analyzed and interpreted, elucidating and completing unknown factors.

DISCUSSION AND ANALYSIS

Lithostratigraphy

In the Ab Kaseh Pass section, the underlying Jurassic sediments (Neyriz and Saraghal formations) rest upon the dolomitic House Kat formation, which is subsequently overlain by thick limestone and reef-building rocks of the Fahliyan formation, dated to the Lower Cretaceous [38]. The Jurassic sedimentary succession has a total thickness of 115 meters, tapering from the base to the top, with bedding angles ranging between 17 to 20 degrees in a northeastern direction. The strata dip at 50 degrees toward the northwest-southeast axis, while the topographic slope varies between 37 to 40 degrees toward the south-southwest. The lithological characteristics of this sequence encompass 18 lithological units, described as follows:

Neyriz Formation

1. Dolomitic limestone: White, porous, with regular layering, with a true thickness of 8.5 meters.
2. Gluconitic shale: Green, weathered, lacking layering with interbeds of chert sandstone, having a thickness of 12 meters.
3. Dolomite: White, porous, exhibiting regular layering, with a thickness of 7.5 meters.
4. Thin-bedded sandstone: Intercalated with silty cream-colored stone, with a thickness of 14 meters.
5. Dark-colored pelitic shales: Durable, thin-bedded, containing fossilized plant remnants and coal streaks, with a thickness of 4 meters.
6. Medium-layered cream-colored dolomite: Fractured, with a thickness of 8 meters.
7. Silty stone: Exhibiting fine layering and clay crack structures, with a thickness of 3 meters.

Saraghal Formation

1. Dark marly shales: Weathered, containing organic matter and lacking layering, with a thickness of 6.5 meters.
2. Thin-bedded dark limestone: Containing chert nodules, with a thickness of 8 meters.
3. Thin-bedded dark silty sandstone: With a thickness of 3 meters.

4. Massive, light-colored, porous dolomite: With a thickness of 6.5 meters.
5. Black oil shale (bituminous): With a thickness of 8 meters (Figure 5-6).
6. Thin-bedded, light gray limestone: Intermixed with bituminous materials, with a thickness of 4.5 meters.
7. Dark shale: Containing petroleum bituminous materials, with a thickness of 5 meters.
8. Gray limestone: Interlayered with black shales, with a thickness of 6.5 meters.
9. Black oil shales (bituminous): With a thickness of 4 meters.
10. Gray silty shale: Impregnated with organic materials, with a thickness of 4 meters.
11. Thin-bedded cream-colored silty stone: With a thickness of 2 meters.

Observations revealed that on top of the last layer of the Saraghal formation, i.e., the thin-bedded cream-colored silty stone, there are red erosive sandstones followed by thick limestone and reef-building rocks, exhibiting colors ranging from cream to light gray, belonging to the Fahliyan formation of Lower Cretaceous age. Based on the lithology type within the studied succession, the stratigraphic column for the above section was illustrated in (Figure 2).

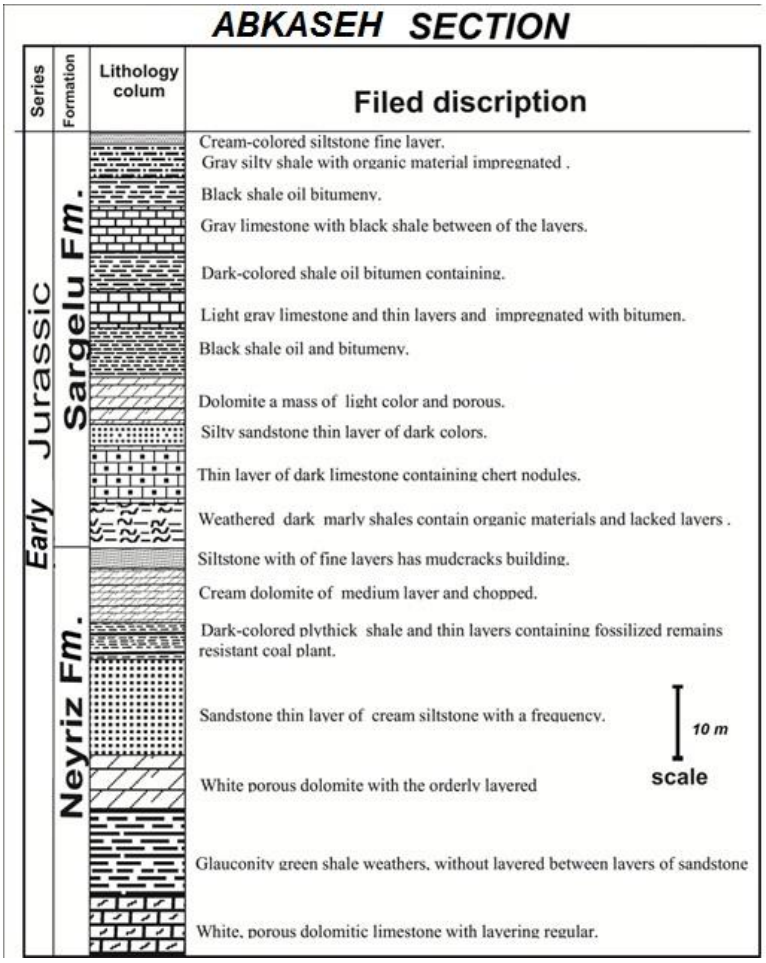

Figure 2. Lithostratigraphic Column of the Ab Kaseh Pass Section

Examination of Plates and Microfacies Atlas - To Determine the Sedimentary Model

A facies is defined as the collection of lithological and paleontological characteristics of a stratigraphic unit that differentiates it from other facies, representing the structural position of the basin, sedimentation conditions, and the biological status of the basin. Lithofacies reflect the physical, mineralogical, and

petrological properties of a stratigraphic unit, while biotic facies present the paleontological characteristics of a stratigraphic unit.

For precise recognition of facies, sedimentological, paleontological, petrological, biological data of fossils, as well as geological and geochemical data, and the nature of the sedimentary environment are examined (Flügel, 2004). Based on studies of the microscopic sections of the sedimentary rocks, the names of the facies are accurately identified, and then each one's position within the basin is delineated, ultimately proposing a sedimentary model for the past basin.

Interpretation of Microfacies in Sedimentary Environmental Conditions for the Studied Sections

Interpretation of Open Marine Facies Belt

Facies studies indicate that the microfacies groups O1 and O2 are deposited in the deep open marine environment of the studied sections. According to laboratory reports, the microfacies groups O1 and O2 are observed in the Saraghal Formation sediments in both sections, with petroleum materials covering the sedimentary particles of these microfacies. The presence of micrite, bioturbation, sponge spicules, and planktonic organisms such as radiolarians suggests that these microfacies are deposited in the deep open marine parts of the outer ramp (Hass & Tardy-Filaz, 2004; Flügel, 2004).

Interpretation of Ramp Facies Belt

This group includes the microfacies R1 and R2, which appear as thin-bedded and occasionally massive limestones in the desert. In microscopic sections, the sorting and rounding of these particles are relatively suitable, with their sizes generally less than 0.05 millimeters. According to laboratory reports, the microfacies groups R1 and R2 are present in the studied sediments of the Saraghal Formation in both sections.

Interpretation of Tidal Flat Microfacies Belt

This belt comprises two facies, T1 and T2, whose formation location corresponds to the tidal flat area and includes low-depth to tidal range sediments of the Saraghal Formation. Similar facies have been reported [39] from southern Tibet and China, and [35] from the Abruzzo region of Italy. Among diagenetic processes affecting this facies, dolomitization can be highlighted, which has occurred extensively in this facies, possibly indicating an initial aragonitic mineralogical signature [1]. According to laboratory findings, the microfacies groups T1 and T2 are observed in the studied sediments of the Saraghal Formation in the Ab Kaseh Pass section, indicating that the main components constituting this facies include peloids (mainly from stone pellets) and diagenetic products, with minor amounts of intraclastic elements. In most of these facies, the components are situated in a framework of sparitic cement.

Analysis of Microfacies in Ab Kaseh Pass Samples

A total of 10 thin-section microfacies samples from the Ab Kaseh Pass were subjected to analysis at the central laboratory of Amirkabir University of Technology, Iran, with the results detailed as follows (Table 1). Subsequently, the lithostratigraphic column for the Ab Kaseh Pass has been constructed using the characteristics and data derived from the microfacies (Figure 3).

In general, to facilitate a better understanding of the sedimentary environment, facies models or depositional models have been proposed (Flügel, 2004). Based on these limited data, it can be interpreted that the absence of barrier reefs, slumping and sliding facies, re-deposited carbonates (Calciturbidite), cortoids, oncoids, peloids, and aggregative grains—which are characteristic of rim-shelf environments—occurs rarely in carbonate ramps [18]. Additionally, the gradual transformation of facies and the expansion of tidal flat areas serve as evidence confirming the sedimentation of this carbonate sequence on a homocline ramp [12].

The depositional model proposed in this study parallels that of the Neotethys Sea, which experienced deposition on homocline ramps from the end of the Triassic [22] to the late Jurassic period [29]. Considering the identified microfossils and examining lateral and vertical changes in facies according to the Wilson and Flügel models (Wilson, 1975; Flügel, 2004), the Jurassic sedimentary environment in the western region of Chaharmahal and Bakhtiari province can be correlated based on similarities. In both samples, this suggests that an open sea environment of the homocline ramp type should be envisioned for predicting the sedimentary environment (Figure 4).

Table 1. Results of Laboratory Microfacies Analysis of the Ab Kaseh Pass Section

AB1	Radiolarian spong spicule wackestone/ Packstone	O_2
AB2	Bioclast Packstone	R_1
AB3	Mixed Packstone/ Grainston	T_2
AB4	Pelloid Bioclast Packstone/ Grainstone	T_1
AB5	Radio larian mudstone/ Wackestone	O_1
AB6	Bioclast Pelloid Wackestone/ Packstone	R_2
AB7	Radiolarian spong spicule wackestone/ Packstone	O_2
AB8	Bioclast Packstone	R_1
AB9	Radiolarian spong spicule wackestone/ Packstone	O_2
AB10	Radio larian mudstone/ Wackestone	O_1

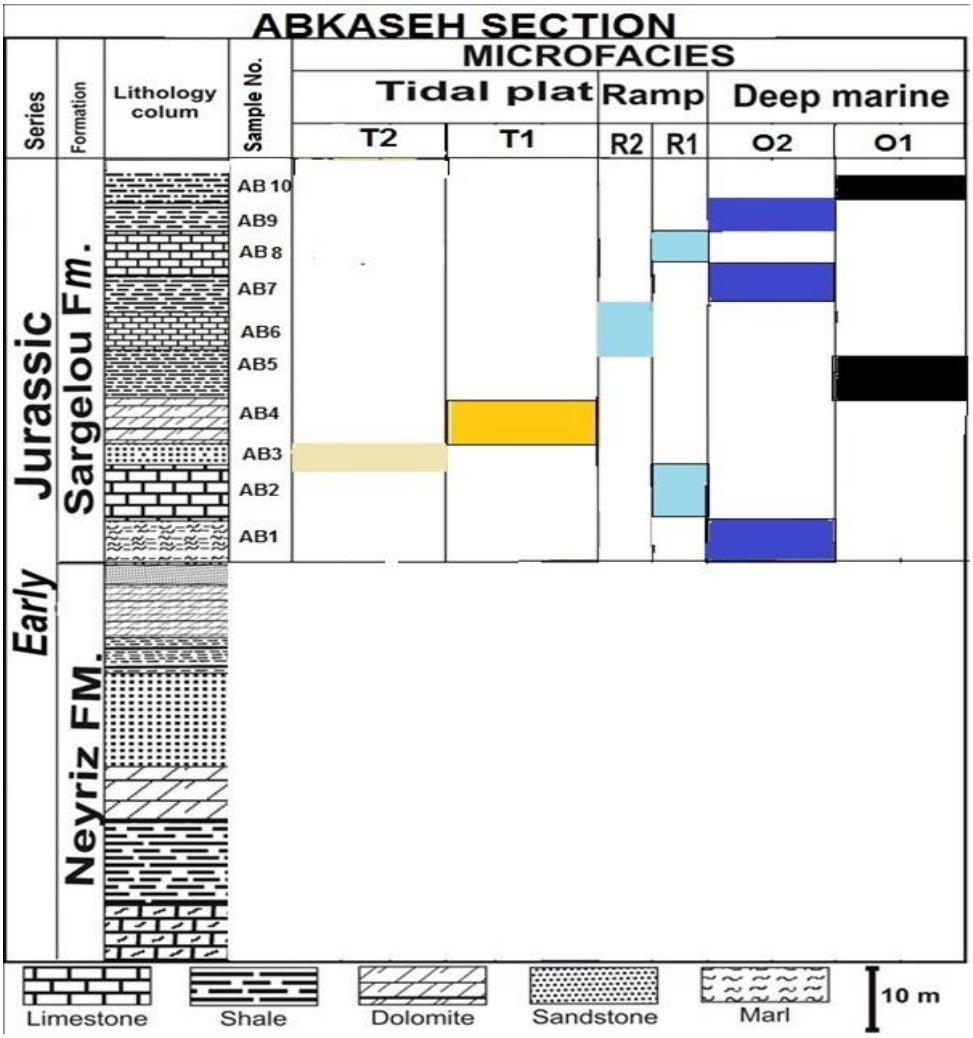

Figure 3. Depiction of Sedimentary Environmental Conditions and Presentation of a Sedimentary Model in the Studied Section

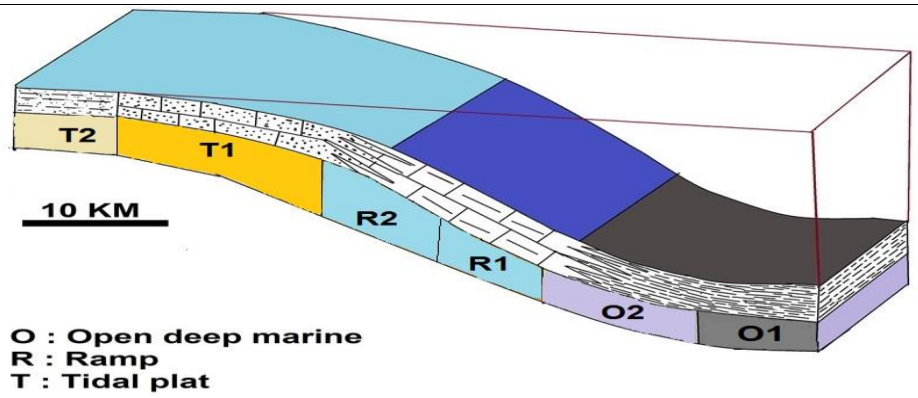

Figure 4. Proposed Basin Model and Sedimentary Environments for the Basin where the Sar-Galu Formation Sediments were Deposited

Rock-Eval Pyrolysis

Functionality of Rock-Eval Pyrolysis

The Rock-Eval pyrolysis technique is used to determine parameters such as Genetic Potential, Production Index, Hydrogen Index (HI), and Oxygen Index (OI). Thus, Rock-Eval pyrolysis assesses the petroleum potential and thermal maturity of oil shales. This method is a standard technique providing valuable information regarding total organic carbon (TOC), the type of organic matter, potential and actual yield, thermal maturity of organic matter, and the type of maturation.

TOC (Total Organic Carbon) is the total amount of organic carbon present, which is calculated using the following formula:

TOC = 0.82 * (S1 + S2) / 10 + S3 / 10

- S1: Represents Free Hydrocarbons, indicating hydrocarbons that are already present and free within the rock. These are released up to 300°C with a heating rate of 5°C per minute, and are measured in mg HC/g rock.

- S2: Represents Oil Potential, which refers to the hydrocarbons generated during pyrolysis between 300-600°C at a heating rate of 25°C per minute. This parameter is also measured in mg HC/g rock. Essentially, the S2 peak represents the current oil potential within the rock sample. Within the temperature range of 300-600°C, the S2 peak is formed by the cracking of kerogen and heavy compounds like resins and asphaltenes.

- S3: Indicates the Organic CO2 Source, representing the oxygen-containing compounds like carboxyl groups that decompose up to 390°C, releasing CO2 gas. This parameter is measured in mg CO2/g rock.

- Tmax: This is the temperature at which the S2 peak reaches its maximum value and is an excellent parameter for evaluating the thermal maturity of a source rock. It is expressed in degrees Celsius.

- HI (Hydrogen Index): Is the ratio of S2 × 100 / TOC.

- OI (Oxygen Index): Is the ratio of S3 × 100 / TOC and is expressed as mg CO2 /g TOC.

Analysis of Rock-Eval Data from Ab Kaseh Pass Oil Shales

As previously mentioned, ten oil shale samples from the Ab Kaseh Pass section were collected and subjected to Rock-Eval pyrolysis analysis. This process provided comprehensive data, and the results for each variable are recorded and presented in detail in Table 2.

Table 2. Data Obtained from Rock-Eval Pyrolysis of Samples from the Ab Kaseh Pass Section

NO. AB	OI	HI	T max	$S_{3}co$(mg/g)	$S_{3'}$ (mg/g)	S_3 (mg/g)	S_2(mg/g)	S_1(mg/g)	TOC
AB1	62	316	436	0.13	5.1	0.53	2.69	0.07	0.85
AB2	19	378	440	0.38	7.8	0.78	15.5	0.32	4.1
AB3	5	467	442	0.35	9.2	0.5	51.56	0.61	11.03
AB4	13	447	445	0.78	14.23	1.99	66.52	1.48	14.89
AB5	10	636	443	0.25	7.01	0.85	54.36	0.45	8.55
AB6	4	513	438	0.22	11.93	0.99	126.3	1.78	24.63
AB7	7	464	439	0.6	12.56	1.54	103.31	1.46	22.25
AB8	11	470	437	1.01	11.9	2.63	116.45	1.6	24.77
AB9	6	496	440	0.69	7.8	1.14	102.3	1.33	20.63
AB10	10	360	445	0.33	8.6	0.68	23.6	0.17	6.55

Source Rock Potential of the Ab Kaseh Pass Section

To determine the Total Organic Carbon (TOC) abundance, a TOC frequency diagram was constructed (Diagram 1). Given that a TOC content above 2 weight percent, as shown in Table 3, indicates a very good source rock for oil shale samples, the oil shale samples from the Ab Kaseh Pass section are therefore classified as excellent source rocks with high oil-generating potential.

Table 3. Classification of Hydrocarbon Source Rocks based on TOC Content [28]

Quantity	TOC in shales (w t%)	TOC in carbonates (w t%)
Poor	0-0.5	0-0.2
Fair	0.5-1	0.2-0.5
Good	1-2	0.5-1
Very good	2-5	1-2
Excellent	>5	>1

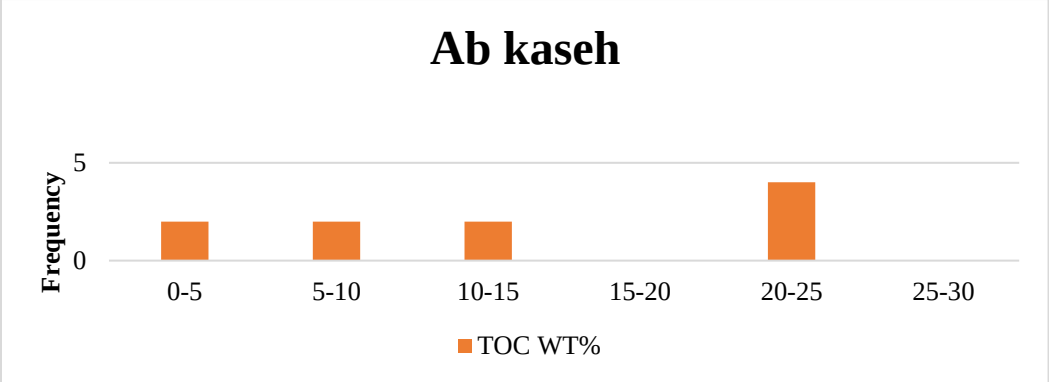

Figure 5. TOC Frequency Diagram of Total Organic Carbon Levels in Oil Shale Samples from the Ab Kaseh Pass Section

Determination of Kerogen Type in the Ab Kaseh Pass Section

To determine the type of kerogen present in the oil shale samples of the Ab Kaseh Pass section, the S2/TOC ratio was used after analysis [19]. As evident from the diagrams, all samples from the Ab Kaseh Pass section are classified as Type II kerogen according to the aforementioned classification.

Therefore, it is noteworthy that the majority of samples from the Ab Kaseh Pass section fall within the range of Type II kerogen, characterized by marine origin and oil-prone potential. According to the Peter standard (Table 4), these samples are rated as very good to excellent in terms of oil-generating potential. The organic matter originates from marine sources, specifically the decomposition of phytoplankton, zooplankton, and marine algae, which were deposited in a strongly reducing environment such as the Tethys Ocean.

Table 4. Standard Parameters for Various Kerogens Defined based on Pyrolysis Analysis by Rock-eval [28]

Kerogen type	HI (mg HC/g TOC)	S2/S3
I	<800	<15
II	300-600	10-15
II/III	200-300	5-10
III	50-200	1-5

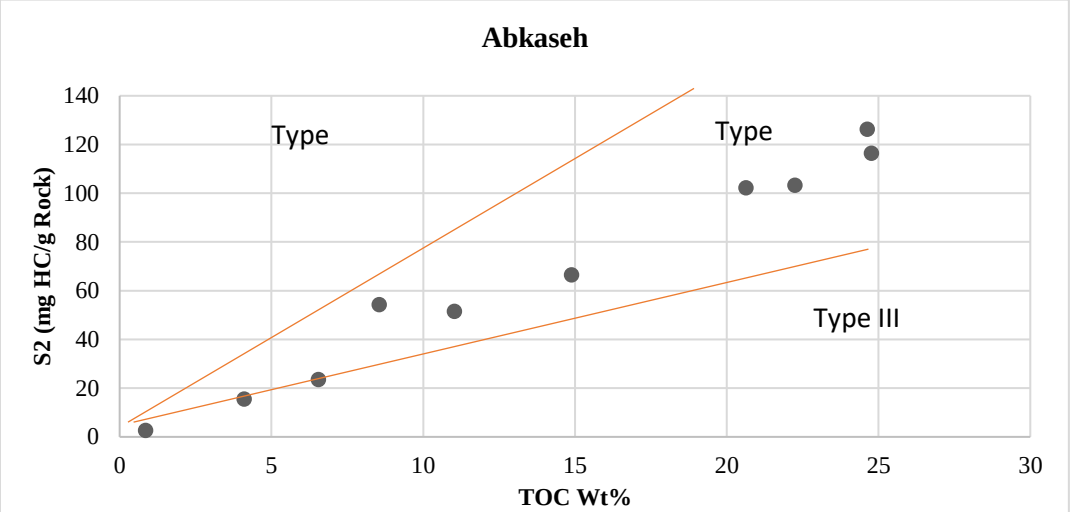

Figure 6. Diagram Determining the Types of Kerogens Present in the Oil Shale Samples from the Ab Kaseh Pass Section

Determination of Thermal Maturity in the Ab Kaseh Pass Section

Using the data obtained from Rock-Eval pyrolysis, a Tmax diagram for the Ab Kaseh Pass section was created (Diagram 3). Based on this diagram and in accordance with the Peter standard (Table 5), the Tmax variable ranges approximately from 440°C to 450°C. This indicates that the oil shale samples from the Ab Kaseh Pass section are at the end of diagenesis and the beginning of thermal maturation, i.e., the initial stage of the oil window. Their range and boundary are depicted as a dark halo on the diagram.

Furthermore, Table 5 provides a pyrolysis guide for the parameters of quantity, quality, and thermal maturity of oil shales. In this table, the position of oil shales can be classified within the range from immature to highly mature, based on both Tmax and the vitrinite reflectance (%Ro). Vitrinite reflectance was not measured in this study. However, the average Tmax obtained from the Rock-Eval analysis of the samples is 439.60°C. By aligning this value with the table, the oil shales from the Ab Kaseh Pass section are positioned within a suitable maturity range in figure 7.

Table 5. Standard Parameters for Evaluating Hydrocarbon Potential based on Thermal Degradation by Rock-eval [28]

Stage of thermal maturity for oil		Maturation
Vitrinite reflectance (R_0%)		Rock-Eval T_{max} (°C)
Immature	0.8-0.2	<435
Mature		
Early	0.6-0.85	435-445
Peak	0.65-0.9	445-450
Late	0.9-1.35	450-470
Post mature	>1.35	>470

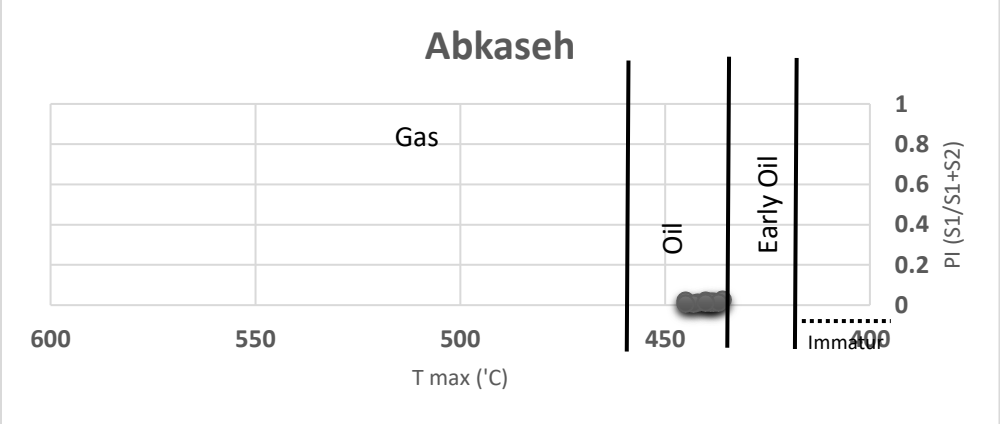

Figure 7. Tmax Diagram and the Positioning of Hydrocarbon Potential in the Samples from the Ab Kaseh Pass Section

Geochemical Analysis Using XRF and ICP Methods

Geochemical Analysis Information Using XRF and ICP Methods After sampling from the studied section, each sample was halved; one half was analyzed using the Rock-Eval apparatus, while the other half, comprising ten samples from the Ab Kaseh Pass section, was sent to reputable geochemical laboratories for XRF and ICP geochemical analyses. The results obtained and collected information for this section are detailed in Table 6. Additionally, the aggregation of the ten samples is presented as averages in Figure 8 and 9.

Table 6. Chemical Analysis Results of Samples from the Ab Kaseh Pass Section using XRF and ICP Methods

Sample No.	AB-1	AB-2	AB-3	AB-4	AB-5	AB-6	AB-7	AB-8	AB-9	AB-10	Average	EF
SiO_2	42.55	50.31	45.58	50.17	43.17	40.33	37.94	40.56	41.72	47.53	43.99	1.31
Al_2O_3	9.34	10.38	10.14	10.66	11.21	10.17	11.30	9.86	8.26	9.47	10.08	1.00
Na_2O	0.16	0.21	0.24	0.12	0.14	0.21	0.21	0.45	0.19	0.18	0.211	0.31
MgO	2.82	2.16	2.11	2.64	2.78	2.33	3.00	2.38	2.77	2.68	2.567	2.15
K_2O	1.73	1.92	1.79	1.56	1.35	1.19	1.91	1.81	1.91	1.99	1.716	0.87
TiO_2	0.74	0.81	0.81	0.84	0.81	0.70	0.85	0.82	0.84	0.81	0.803	1.60
MnO	0.04	0.07	0.07	0.05	0.08	0.06	0.07	0.08	0.08	0.06	0.066	1.12
CaO	9.70	9.11	9.79	9.33	9.17	9.93	9.87	9.99	9.88	9.83	9.66	13.97
P_2O_5	0.11	0.19	0.14	0.25	0.21	0.31	0.22	0.32	0.16	0.21	0.212	2.38
Fe_2O_3	7.13	7.88	7.78	7.92	9.19	7.96	6.98	7.88	7.34	8.16	7.822	2.02
TOC	0.85	4.1	11.03	14.89	8.55	24.63	22.25	24.77	20.63	6.55	13.82	-
Ba	241	253	260	256	235	265	248	246	253	253	251.0	0.78
Ce	63	66	70	67	61	67	66	67	67	70	66.4	1.50
Co	8	9	11	7	9	10	9	9	9	10	9.1	0.74
Cr	143	148	150	141	155	160	157	153	144	154	150.5	2.80
Cu	24	31	19	26	25	31	29	28	29	26	26.8	1.00
Nb	13	12	16	15	16	17	16	12	14	17	14.8	1.42
Mo	5	5	7	4	7	7	8	7	6	4	6.0	-
U	8	9	6	7	7	6	10	9	7	8	7.7	4.66
Th	4	6	6	3	6	5	6	6	7	5	5.4	0.71
Cd	110	108	114	109	122	119	116	108	114	112	113.2	-
Ni	132	139	142	142	144	143	141	136	142	137	139.8	4.72
Pb	13	12	116	16	17	14	16	15	17	15	15.1	1.40
Rb	62	69	64	61	68	65	69	68	68	68	66.2	0.75
Sr	405	411	413	418	413	408	412	413	400	413	410.6	3.85
V	105	108	108	110	115	109	112	109	125	107	110.8	1.33
W	4	5	6	3	5	4	6	6	4	5	4.8	3.33
Y	18	19	13	21	21	20	15	22	16	16	18.1	1.26
Zr	107	113	109	109	101	113	115	112	115	114	110.8	1.00
Zn	94	91	98	94	96	97	88	90	96	96	94.0	2.00

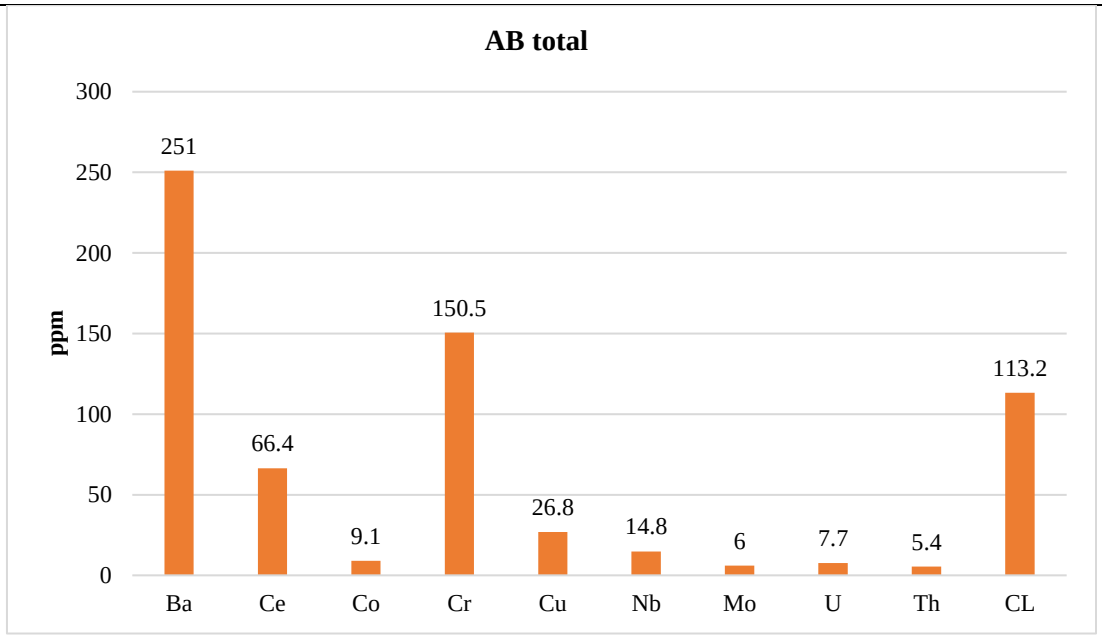

Figure 8. Geochemical Analysis of Samples from the Ab Kaseh Pass Section Presented as Aggregated Averages for Trace Elements

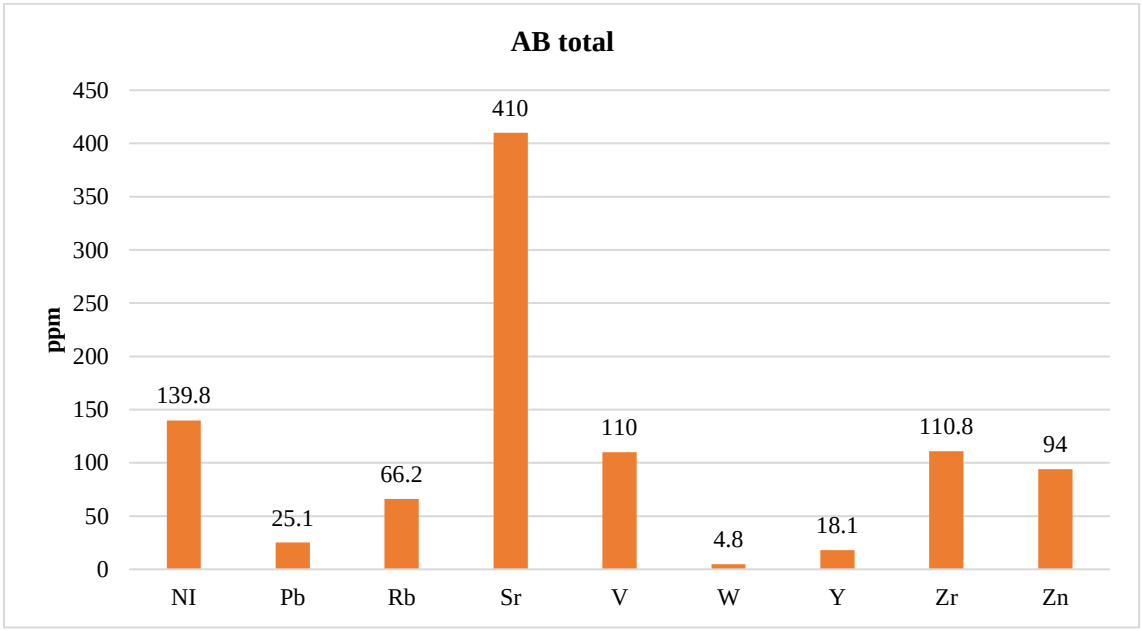

Figure 9. Geochemical analysis of samples from the Ab Kaseh Pass section presented as aggregated results for heavy metals

Analysis of Geochemical Data Using XRF and ICP Methods

The quantities obtained from the oil shales in this section indicate their richness in trace elements, heavy elements, and metallic and non-metallic oxides (in some elements). Therefore, the oil shales in this area of the Central Zagros hold dual economic value: one due to a high unconventional oil reserve and the other due to the elevated levels of certain trace elements and heavy metals, or generally valuable metallic and non-metallic elements stored within these oil shales.

The organic matter content and enrichment of trace elements in the oil shales are influenced by their mineralogy [26][24]. The study of thin sections of the Sar-Galu Formation samples from the Ab Kaseh Pass section reveals that carbonate minerals are the primary constituents. The results of the chemical

analysis of these samples also indicate the predominance of SiO2, CaO, and Al2O3 oxides, confirming the abundance of carbonates along with clay minerals and quartz [32].

Organic matter, detrital materials, seawater, submarine volcanism, and biogenic materials can serve as sources of elements in oil shales. In the Sar-Galu Formation, elements such as Sr and P may have a biogenic origin. The elements Ti, Al, and Si, which form oxide and clay minerals, are of detrital origin. The origins of the elements Ni, U, W, and Cr are attributed to organic matter and adsorption onto clay minerals. The formation of phosphates via biological processes in marine environments has been studied. In reducing environments, phosphatic minerals also form at the interface between water and sediment. Furthermore, organic matter positively influences phosphate adsorption [14][37][34]. The element P exhibits a positive correlation in the Ab Kaseh Pass section, as shown in Table 7 and Figure 6. Thus, a biogenic origin for P is confirmed, at least in the Ab Kaseh Pass section. The origin of the element Sr may be both carbonate and biogenic. Given that Sr shows a negative correlation with TOC in the Ab Kaseh Pass section, it appears that its origin is not biogenic. The element Sr has a negative correlation in the Ab Kaseh Pass section as indicated in Table 7 and Figure 6. The element Ni shows a positive correlation with TOC in the Ab Kaseh Pass section, while the elements W and Cr also show positive correlations in this section. This may indicate that the origin of these elements is organic matter. In other words, the increase in the concentration of these elements likely results from environmental enrichment due to organic matter [32]. The element U in the Ab Kaseh Pass section shows no correlation. As shown in Table 7 and Figure 10, U exhibits a negative correlation with both SiO2 and Al2O3 in the Ab Kaseh Pass section. Therefore, the origin of U cannot be definitively determined, but it likely involves organic matter and clay minerals contributing to its enrichment.

Due to the negligible enrichment or depletion of other elements in the samples studied from the Ab Kaseh Pass section, their origins have not been analyzed.

Table 7. Correlation Coefficients of Major Oxides and Trace Elements in the Sar-Galu Formation at the Ab Kaseh Pass Section

	Zn	Zr	Y	W	V	Sr	Rb	Pb	Ni	Cd	Th	U	Mo	Nb	Cu	Cr	Co	Ce	Ba
Zn	1.00																		
Zr	-0.32	1.00																	
Y	-0.19	-0.35	1.00																
W	-0.36	0.11	-0.35	1.00															
V	0.12	0.12	-0.09	-0.16	1.00														
Sr	-0.19	-0.26	0.25	0.22	-0.49	1.00													
Rb	-0.38	0.36	-0.09	0.59	0.36	-0.13	1.00												
Pb	0.24	-0.18	-0.18	0.07	0.66	0.09	0.08	1.00											
Ni	0.32	-0.09	-0.03	-0.07	0.52	0.17	0.13	0.59	1.00										
Cd	0.40	-0.33	-0.09	0.07	0.36	-0.12	0.20	0.49	0.65	1.00									
Th	-0.08	0.25	-0.33	0.62	0.56	-0.40	0.80	0.26	0.27	0.30	1.00								
U	-0.93	0.35	0.03	0.43	-0.15	0.11	0.52	-0.28	-0.47	-0.41	0.15	1.00							
Mo	-0.19	-0.02	-0.13	0.61	0.25	-0.11	0.37	0.33	0.37	0.57	0.60	0.06	1.00						
Nb	0.50	-0.04	-0.34	-0.02	0.02	0.22	-0.07	0.45	0.54	0.70	-0.11	-0.45	0.16	1.00					
Cu	-0.46	0.55	0.40	-0.19	0.25	-0.25	0.48	-0.31	0.08	-0.03	0.17	0.39	0.04	-0.21	1.00				
Cr	-0.06	0.12	0.00	0.54	-0.12	0.16	0.52	0.06	0.28	0.61	0.35	0.08	0.63	0.52	0.26	1.00			
Co	0.40	0.21	-0.54	0.60	-0.06	-0.09	0.36	0.05	0.22	0.37	0.57	-0.28	0.43	0.43	-0.21	0.61	1.00		
Ce	0.18	0.66	-0.49	0.18	-0.14	0.16	-0.01	0.04	0.04	-0.33	0.05	-0.14	-0.17	0.24	-0.11	0.05	0.50	1.00	
Ba	0.32	0.57	-0.28	-0.18	-0.09	0.02	-0.23	-0.13	0.33	-0.09	-0.09	-0.43	-0.09	0.32	0.14	0.08	0.39	0.77	1.00
SiO_2	0.21	-0.13	0.08	-0.32	-0.28	0.43	-0.26	-0.26	-0.01	-0.47	-0.39	-0.16	-0.79	-0.12	-0.18	-0.50	-0.18	0.24	0.21
Al_2O_3	-0.35	-0.37	0.23	0.28	-0.30	0.72	0.05	0.07	0.39	0.32	0.55	-0.36	0.26	0.04	-0.35	0.04	0.15	-0.22	-0.17
CaO	0.02	0.55	-0.36	0.26	0.04	-0.35	0.04	0.15	-0.22	0.02	0.20	-0.00	0.35	0.19	0.00	0.31	0.40	0.49	0.31
Na_2O	-0.40	0.30	0.17	0.61	-0.13	0.05	0.34	-0.10	-0.29	-0.32	0.40	0.33	0.42	-0.44	0.12	0.29	0.28	0.27	0.02
MgO	-0.23	-0.08	-0.05	-0.20	0.35	-0.20	0.06	0.40	-0.09	0.26	-0.12	0.32	-0.00	0.19	0.08	-0.07	-0.48	-0.44	-0.56
K_2O	-0.40	0.53	-0.54	0.40	0.03	-0.11	0.37	-0.08	-0.45	-0.59	0.31	0.59	-0.23	-0.37	-0.05	-0.30	0.07	0.42	-0.07
TiO_2	-0.39	0.15	-0.20	0.28	0.43	0.31	0.36	0.55	0.21	-0.22	0.29	0.40	-0.01	-0.14	-0.08	-0.26	-0.20	0.17	-0.21
MnO	-0.12	0.09	-0.01	0.57	0.59	-0.06	0.77	0.46	0.46	0.31	0.88	0.11	0.58	-0.07	0.18	0.37	0.40	0.02	-0.14
P_2O_5	-0.26	0.21	0.63	0.04	-0.08	0.39	0.18	0.03	0.23	0.06	-0.08	0.08	0.23	0.10	0.52	0.53	-0.03	0.12	0.23
Fe_2O_3	0.40	-0.61	0.48	0.00	0.00	0.44	0.14	0.22	0.40	0.41	0.02	-0.37	-0.05	0.27	-0.12	0.30	0.14	-0.24	-0.22
TOC	-0.21	0.46	0.13	0.12	0.40	-0.05	0.20	0.41	0.40	0.21	0.27	-0.00	0.58	0.15	0.42	0.40	0.10	0.25	0.35

	SiO_2	Al_2O_3	CaO	Na_2O	MgO	K_2O	TiO_2	MnO	P_2O_5	Fe_2O_3	TOC
SiO_2	1.00										
Al_2O_3	0.02	1.00									
CaO	-0.65	-0.45	1.00								
Na_2O	-0.36	-0.12	0.50	1.00							
MgO	-0.39	0.02	0.08	-0.40	1.00						
K_2O	0.16	-0.36	0.18	0.23	0.08	1.00					
TiO_2	0.19	0.13	-0.17	0.07	0.25	0.59	1.00				
MnO	-0.28	0.06	0.04	0.46	-0.15	0.13	0.47	1.00			
P_2O_5	-0.20	0.31	0.19	0.47	-0.17	-0.41	-0.09	0.23	1.00		
Fe_2O_3	0.31	0.35	-0.51	-0.11	-0.20	-0.50	-0.04	0.31	0.29	1.00	
TOC	-0.60	0.03	0.58	0.48	0.02	-0.20	0.10	0.42	0.69	-0.19	1.00

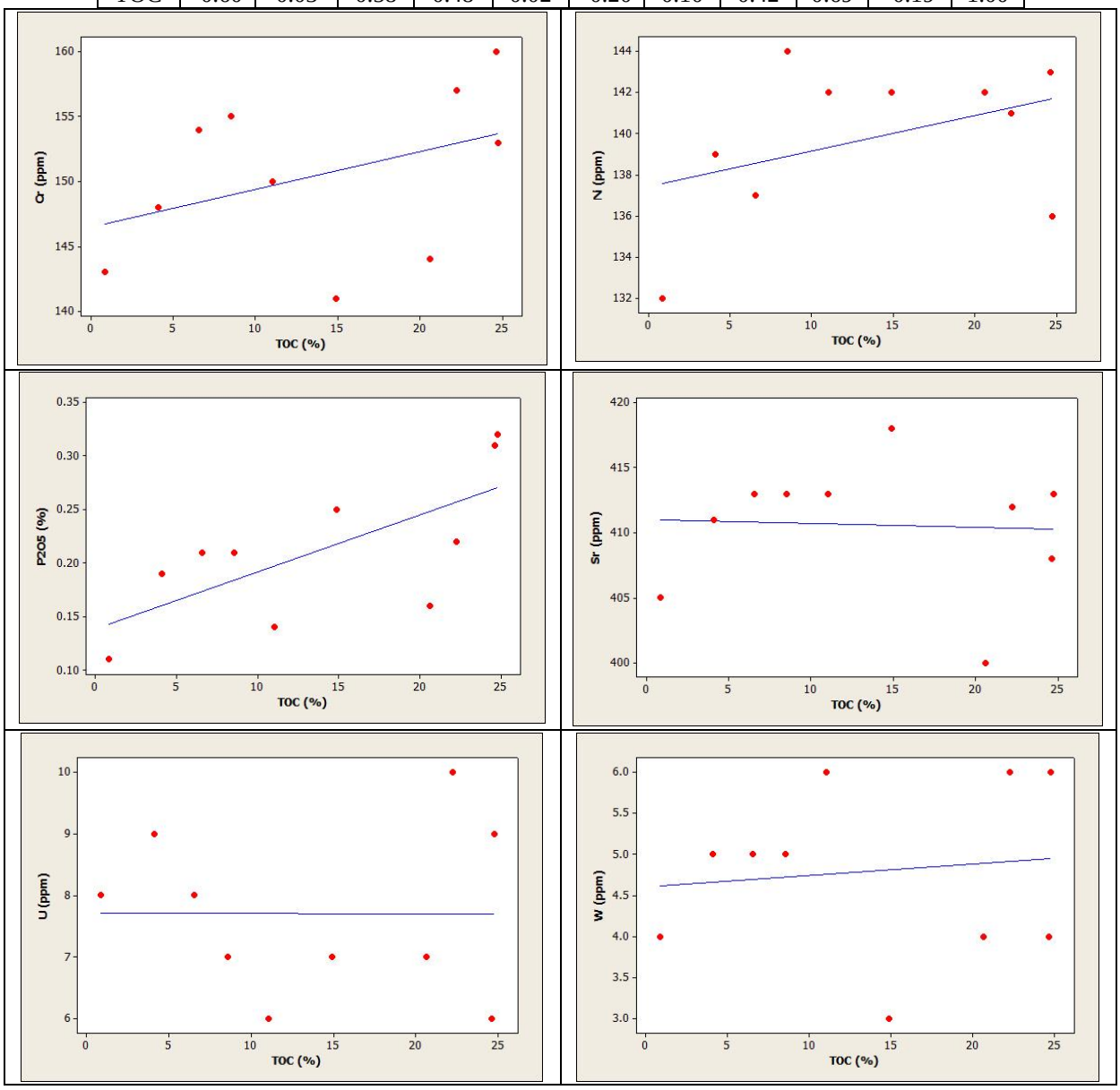

Figure 10. Correlation Diagrams of P2O5, Sr, Ni, W, Cr, and U with TOC in Samples of the Sar-galu Formation from the Ab Pass Section

RESULTS

1. Geological studies have indicated that the oil shale deposits in the Ab Kaseh Pass section belong to the Sar-Galu Formation, which was deposited in a homoclinal ramp within the Tethys Sea territory, with a total of six microfacies identified from three sedimentary environment belts.

2. The age of the deposits in the Ab Kaseh Pass section has been determined to be Lower Jurassic (Early Jurassic) through the analysis of index foraminifera microfossils.

3. Based on microfacies analysis, it is concluded that the Jurassic sediments of the Zagros in this region (Central Zagros) were formed in an open marine setting of a homoclinal ramp. Concurrently, in deeper areas, the shale deposits of the Sar-Galu Formation were formed, while in shallow ramp areas and intertidal zones, limestone and sandy sediments were deposited.

4. The investigations reveal that the lack of maturity of the Sar-Galu Formation oil shales is attributed to the tectonic conditions of the basin. The activity of regional [4] faults and the uplift of the basin due to Jurassic orogenic activities hindered the deposition of overlying Upper Jurassic sediments on the shales, resulting in insufficient deep heating for the maturation of the oil shales. Consequently, these shales have remained immature and have lost the conditions necessary for oil generation.

5. In the Ab Kaseh Pass section, the deposits of the Sar-Galu Formation primarily consist of clay, marl, limestone, and oil shale, with these facies exhibiting interdigitating characteristics.

6. The investigations show that the lower boundary of the Sar-Galu Formation with the Nyriz Formation deposits is continuous and gradual, while the upper boundary of this formation with the Fahliyan Formation limestones is discontinuous (unconformable) with a Lower Cretaceous age, and the Upper Jurassic deposits are absent.

7. Considering that a TOC content higher than 2% by weight indicates a very good source rock for oil shale samples [28], the weight percentage of TOC for the studied section is significantly high, placing it in the category of excellent oil-prone source rock.

8. Diagrams defining the types of kerogen in shale samples from both sections were constructed based on the ratio of TOC to S2, and it is evident from the diagrams that, according to the above classification, all samples from the Ab Kaseh Pass section contain Type II kerogen.

9. Utilizing the data obtained from Rock-Eval pyrolysis and Tmax diagrams in the Ab Kaseh Pass section, the Tmax variable ranges from approximately 440 degrees to 450 degrees, indicating that the oil shale samples in the Ab Kaseh Pass section lie at the end of diagenesis and the beginning of thermal maturation, which corresponds to the early stage of the oil window.

10. Based on the resulting HI values from the Ab Kaseh Pass section and their comparison with standard tables, it was determined that the type of hydrocarbon produced from the shale samples in the studied section is solely crude oil, with no gas generation.

11. The presence of significant concentrations of trace heavy metals within these shales suggests that their origin could be derived from the oceanic crust of the Tethys Sea, which was in a rifting (oceanic formation) phase during the Jurassic period. Since the Sar-Galu shales were deposited in the deep marine environment, these elements have been adsorbed by organic matter. Additionally, these elements may also have a detrital origin due to proximity to the Sanandaj-Sirjan zone, from which detrital materials entered the Tethys basin during weathering and erosion.

12. Thin sections of the Sar-Galu Formation samples from the Ab Kaseh Pass indicate that carbonate minerals are the primary constituents. Simultaneously, the results of chemical analyses of metallic and non-metallic oxides also show that oxides such as SiO2, CaO, and Al2O3 dominate in the studied oil shales, confirming the abundance of carbonates in this section.

13. The element P in the Ab Kaseh Pass section shows a positive correlation. Therefore, the biogenic origin of P in this section is confirmed.

14. Considering that Sr exhibits a negative correlation with TOC in the Ab Kaseh Pass section according to the diagrams and correlation coefficients, its origin does not appear to be biogenic.

15. The element Ni shows a positive correlation with TOC in the Ab Kaseh Pass section, and the elements W and Cr also exhibit positive correlations. This may indicate that the origin of these elements is organic matter. In other words, the increase in the concentrations of these elements is likely a result of environmental enrichment by organic matter.

16. The element U in the Ab Kaseh Pass section shows no correlation. In this section, U has a negative correlation with both SiO2 and Al2O3. Therefore, the origin of U cannot be definitively determined, although it is likely that organic matter and clay minerals have contributed to its enrichment.

REFERENCES

[1] Adabi MH, Mehmandosti EA. Microfacies and geochemistry of the Ilam Formation in the Tang-E Rashid area, Izeh, SW Iran. Journal of Asian Earth Sciences. 2008 Jul 15;33(3-4):267-77.

[2] Adabi MH, Rao CP. Petrographic and geochemical evidence for original aragonite mineralogy of Upper Jurassic carbonates (Mozduran Formation), Sarakhs area, Iran. Sedimentary Geology. 1991 Aug 1;72(3-4):253-67.

[3] Yağız E, Ozyilmaz G, Ozyilmaz AT. Optimization of Graphite-Mineral Oil Ratio with Response Surface Methodology in Glucose Oxidase Based Carbon Paste Electrode Design. Natural and Engineering Sciences. 2022 Apr 1;7(1):22-33. http://doi.org/10.28978/nesciences.1098655

[4] Alavi M. Regional stratigraphy of the Zagros fold-thrust belt of Iran and its proforeland evolution. American journal of Science. 2004 Jan 1;304(1):1-20.

[5] Alavi M. Tectonostratigraphic evolution of the Zagrosides of Iran. Geology. 1980 Mar 1;8(3):144-9. https://doi.org/10.1130/0091-7613(1980)8%3C144:TEOTZO%3E2.0.CO;2

[6] Salkić Z, Babajić E, Lugović B. Geochemistry and petrogenesis of Oligocene dacites from the Central Bosnia and Herzegovina with insight in the post-collisional tectonic evolution of Central Dinaridic Ophiolite Belt. Archives for Technical Sciences. 2021(24):17-30. https://doi.org/10.7251/afts.2021.1324.017S

[7] Alavi M. Tectonic Map of the Middle East, Scale 1: 5,000,000: Geological. Surv. Iran. 1991.

[8] Alavi M. Tectonics of the Zagros orogenic belt of Iran: new data and interpretations. Tectonophysics. 1994 Jan 30;229(3-4):211-38. https://doi.org/10.1016/0040-1951(94)90030-2

[9] Alavi M. Structures of the Zagros fold-thrust belt in Iran. American Journal of science. 2007 Nov 1;307(9):1064-95. https://doi.org 10.2475/09.2007.02

[10] Leiwi AAA. The Repercussions of Oil Price Fluctuations on Iraq's Gross Domestic Product Analytical Study for the Period between 2000-2019. IAJAFM [Internet]. 2022 Oct. 18 [cited 2025 Feb. 24];9(2):48-61. https://doi.org/10.9756/IAJAFM/V9I2/IAJAFM0906

[11] Berberian M. Contribution to the seismotectonics of Iran. 3. na; 1977.

[12] Berberian M. Master "blind" thrust faults hidden under the Zagros folds: active basement tectonics and surface morphotectonics. Tectonophysics. 1995 Jan 30;241(3-4):193-224.

[13] Atti LM. The effect of ethical behavior strategy on job voice, work ethics as an interactive variable: An applied study in the Basra South Oil Company. Int Acad J Organ Behav Hum Resour Manag. 2024;11(1):1-1. https://doi.org/10.9756/IAJOBHRM/V11I1/IAJOBHRM1101

[14] Boggs Jr S. Petrology of sedimentary rocks. Cambridge university press; 2009 Feb 19.

[15] Dunham RJ. Classification of carbonate rocks according to depositional texture. 1962.

[16] Mahmeed A-OSM. Evaluate the continuous improvement of operations according to the business continuity model (ISO 22301: 2019) a case study: The General Company for Vegetable Oils. Int Acad J Bus Manag. 2023;10(1):81-98. https://doi.org/10.9756/IAJBM/V10I1/IAJBM1008

[17] Fereidoni M, Lotfi M, Rashid Nejad N, Rashidi M. Evaluate geochemical trace elements of Qalikuh oil shale (Southwest Aligoodarz) using elemental analysis and rock eval pyrolysis. Scientific Quarterly Journal of Geosciences. 2016 Mar 1;25(98):171-80. https://doi.org/10.22071/gsj.2016.41188

[18] Flügel E. Microfacies analysis of limestones. Springer Science & Business Media; 2012 Dec 6.

[19] Flügel E. Microfacies of carbonate rocks. Berlin: Springer Verlag; 2000.

[20] Jumaah AA, Majeed HS. The International Energy Agency and its role in the global oil market. Int Acad J Econ. 2023;10(1):54-63. https://doi.org/10.9756/IAJE/V10I1/IAJE1006

[21] Hakimi MH, Abdullah WH, Alqudah M, Makeen YM, Mustapha KA. Organic geochemical and petrographic characteristics of the oil shales in the Lajjun area, Central Jordan: Origin of organic matter input and preservation conditions. Fuel. 2016 Oct 1;181:34-45. https://doi.org/10.1016/j.fuel.2016.04.070

[22] Haas J, Tardy-Filácz E. Facies changes in the Triassic–Jurassic boundary interval in an intraplatform basin succession at Csővár (Transdanubian Range, Hungary). Sedimentary Geology. 2004 Jun 1;168(1-2):19-48. https://doi.org/10.1016/j.sedgeo.2004.03.002

[23] Đurić N, Đurić M. Research of marly rocks on the terrain forecasted for construction of silos objects. Archives for Technical Sciences. 2023 Nov 27;2(29):1-9. https://doi.org/10.59456/afts.2023.1529.001Dj

[24] Jiang Z, Zhang W, Liang C, Wang Y, Liu H, Chen X. Basic characteristics and evaluation of shale oil reservoirs. Petroleum Research. 2016 Dec 1;1(2):149-63. https://doi.org/10.1016/S2096-2495(17)30039-X

[25] Makeen YM, Abdullah WH, Ayinla HA, Shan X, Liang Y, Su S, Noor NM, Hasnan HK, Asiwaju L. Organic geochemical characteristics and depositional setting of Paleogene oil shale, mudstone and sandstone from onshore Penyu Basin, Chenor, Pahang, Malaysia. International Journal of Coal Geology. 2019 Apr 15;207:52-72. https://doi.org/10.1016/j.coal.2019.03.012

[26] McQuarrie N. Crustal scale geometry of the Zagros fold–thrust belt, Iran. Journal of structural Geology. 2004 Mar 1;26(3):519-35. https://doi.org/10.1016/j.jsg.2003.08.009

[27] Mohajjel M, Fergusson CL, Sahandi MR. Cretaceous–Tertiary convergence and continental collision, Sanandaj–Sirjan zone, western Iran. Journal of Asian Earth Sciences. 2003 Jan 1;21(4):397-412. https://doi.org/10.1016/S1367-9120(02)00035-4

[28] Peters KE, Cassa MR. Applied source rock geochemistry. https://doi.org/10.1306/M60585C5

[29] Pomar L, Hallock P. Carbonate factories: a conundrum in sedimentary geology. Earth-Science Reviews. 2008 Mar 1;87(3-4):134-69. https://doi.org/10.1016/j.earscirev.2007.12.002

[30] Rahimi D. Potential ground water resources:(Case study: Shahrekord plain).

[31] Rasouli A, Shekarifard A, Farahani FJ, Kök MV, Daryabandeh M, Rashidi M. Occurrence of organic matter-rich deposits (Middle Jurassic to Lower Cretaceous) from Qalikuh locality, Zagros Basin, South–West of Iran: A possible oil shale resource. International Journal of Coal Geology. 2015 Apr 1;143:34-42. https://doi.org/10.1016/j.coal.2015.03.010

[32] Scott RW. Global environmental controls on Cretaceous reefal ecosystems. Palaeogeography, Palaeoclimatology, Palaeoecology. 1995 Dec 1;119(1-2):187-99. https://doi.org/10.1016/0031-0182(94)00068-9

[33] Selly RC. Ancient sedimentary environments and their subsurface diagnosis. London: Chapman and Hall; 1996.

[34] Slansky M. Geology of sedimentary phosphates. 1986

[35] Stossel I. Rudist and carbonate platform evaluation: the Late Cretaceous Maiella carbonate platform margin (Abruzzi, Italy). Mem Sci Geol. 1999;51:333-41.

[36] Stössel I, Bernoulli D. Rudist lithosome development on the Maiella Carbonate Platform margin. https://doi.org/10.1144/GSL.SP.2000.178.01.12

[37] Tzifas IT, Godelitsas A, Magganas A, Androulakaki E, Eleftheriou G, Mertzimekis TJ, Perraki M. Uranium-bearing phosphatized limestones of NW Greece. Journal of Geochemical Exploration. 2014 Aug 1;143:62-73. https://doi.org/10.1016/j.gexplo.2014.03.009

[38] Wilkerson CL. Trace metal composition of Green River retorted shale oil. Fuel. 1982 Jan 1;61(1):63-70. https://doi.org/10.1016/0016-2361(82)90294-0

[39] Zhicheng Z, Willems H, Binggao Z. Cretaceous-Paleogene biofacies and ichnofacies in southern Tibet. Wei ti gu Sheng wu xue bao= Acta Micropalaeontologica Sinica. 1998 Jan 1;15(3):307-17.